

New narrow nucleon resonances $N^*(1685)$ and $N^*(1726)$ within the chiral quark-soliton model

Ghil-Seok Yang^{1,*} and Hyun-Chul Kim^{2,3,4,†}

¹*Department of Physics, Soongsil University, Seoul 06978, Republic of Korea*

²*Department of Physics, Inha University, Incheon 22212, Republic of Korea*

³*Advanced Science Research Center, Japan Atomic Energy Agency, Shirakata, Tokai, Ibaraki, 319-1195, Japan*

⁴*School of Physics, Korea Institute for Advanced Study (KIAS), Seoul 02455, Republic of Korea*

(Dated: July 18, 2019)

We investigate the strong and radiative decay widths of the narrow nucleon resonances $N^*(1685)$ and $N^*(1726)$ within the framework of the SU(3) chiral quark-soliton model. All the relevant parameters are taken from those used to describe the properties of the baryon octet and decuplet in previous works. The masses of the antidecuplet nucleon and the eikosiheptaplet (27-plet) nucleon with spin 3/2 are determined respectively to be (1690.2 ± 10.5) MeV and (1719.6 ± 7.4) MeV. The decay width for $N^*(1685) \rightarrow \eta + N$ is found to be approximately three times larger than that for $N^*(1685) \rightarrow \pi + N$. The width of the decay $N^*(1726) 3/2^+ \rightarrow \eta + N$ is even about 31 times larger than that of $N^*(1726) 3/2^+ \rightarrow \pi + N$. The ratio of the radiative decays for $N^*(1685)$ is obtained to be $\Gamma_{nn^*(1685)}/\Gamma_{pp^*(1685)} = 8.62 \pm 3.45$ which explains very well the neutron anomaly. In contrast, we find $\Gamma_{pp^*(1726)}/\Gamma_{nn^*(1726)} = 3.72 \pm 0.64$, which indicates that the production of $N^*(1726)$ is more likely to be observed in the proton channel. We also examined the decay modes of these narrow nucleon resonances with the strangeness hadrons involved.

PACS numbers: 13.30.Eg, 13.60.Rj, 14.20.-c, 14.20.Gk, 14.20.Pt

Keywords: narrow nucleon resonances, hadronic decays, exotic baryons, pentaquarks, the chiral quark-soliton model

arXiv:1809.07489v3 [hep-ph] 17 Jul 2019

* E-mail: ghsyang@ssu.ac.kr

† E-mail: hchkim@inha.ac.kr

I. INTRODUCTION

Since Kuznetsov et al. announced the finding of a narrow nucleon resonance or a narrow bump-like structure around the center of mass energy $W \sim 1.68$ GeV in photoproduction of η mesons off the quasi-free neutron [1], several experimental collaborations have subsequently confirmed its existence [2–7]. The broad nucleon resonance $N(1535, 1/2^-)$ appears as the dominant one in η photoproduction off the nucleon, so that this narrow state was placed on the shoulder of the $N(1535, 1/2^-)$ in the vicinity of $W \sim 1.68$ GeV. On the other hand, it was experimentally shown that such a narrow structure does not exist for the proton [3, 8] or seems to have a dip-like structure for the proton [4, 9]. Recently, A2 Collaboration has measured the double polarization observable and the helicity-dependent cross sections for η photoproduction from the quasi-free protons and neutrons [10], using a circularly polarized photon beam. The narrow structure was observed only in the spin-1/2 helicity-dependent cross section, which indicates that a spin-1/2 amplitude is most likely related to this narrow structure. Reference [10] concluded that this structure is unambiguously related to the helicity-1/2 amplitude. Moreover, the experimental data being compared with different model predictions of the angular dependence, a narrow structure is favored to be interpreted as a narrow P_{11} nucleon resonance. The pronounced bump-like structure found only for the neutron is often called *neutron anomaly* [11].

As the narrow bump-like structure was undisputably established by several experiments, there has been various theoretical interpretations of it. Shklyar et al. [12] explained that it comes from the coupled-channel effects due to $N(1650)1/2^-$ and $N(1710)1/2^+$ based on the unitary coupled-channels effective Lagrangian approach, while Shyam and Scholten [13] described it as the interference effects of $N(1535)1/2^-$, $N(1650)1/2^-$, $N(1710)1/2^+$, and $N(1720)3/2^+$ resonance contributions, using a coupled-channels K -matrix method. Anisovich et al. [14, 15] interpreted that the narrow bump-like structure arises from the interference between the $N(1535)1/2^-$ and the $N(1650)1/2^-$. On the other hand, Döring and Nakayama [16] studied the ratio of the cross section σ_n/σ_p with the intermediate meson-baryon states with strangeness and interpreted the pronounced narrow structure as the effects coming from the opening of the strangeness channel in intermediate states. On the contrary, Refs. [17–19] explained the $\gamma n \rightarrow \eta n$ reaction very well within an Effective Lagrangian approach, regarding the narrow structure as the narrow nucleon resonance $N^*(1685)1/2^+$. In particular, Suh et al. [19] was able to describe the precise experimental data on the helicity-dependent cross sections from the A2 Collaboration [10]. Kuznetsov et al. [11] analyzed the GRAAL data and found also the evidence of a narrow structure in the Σ beam asymmetry for the reaction $\gamma p \rightarrow \eta p$ and argued that the evidence of the narrow structure in the proton channel cannot be explained by those coupled-channel effects. In a more recent work [20], Kuznetsov et al. refuted that interpretation of the pronounced narrow bump-like structure as an interference effect between the S -wave nucleon resonances. The key point of Ref. [20] is that the signal of $N^*(1685)$ may appear in polarization observables for η photoproduction off the proton even if this resonance has a weaker transition magnetic moments than that of the neutron. We also want to mention that both the narrow excited proton and neutron were also seen in Compton scattering $\gamma N \rightarrow \gamma N$ [21, 22] and the reactions $\gamma N \rightarrow \pi \eta N$ [23].

In the meanwhile, the second narrow peak around $W \sim 1.72$ GeV was seen in several different experiments. The beam asymmetry for η photoproduction off the proton [10] gave a hint for the existence of the second narrow resonance. That for Compton scattering on the proton exhibited also it together with the first bump-like structure [22]. Gridnev et al. [24] performed the high-precision analysis of the $\pi^\pm p$ cross-sectional data from the EPECUR Collaboration based on the multi-channel K -matrix approach and found both the narrow structures at $W \sim 1.68$ GeV and $W \sim 1.72$ GeV, respectively. What is interesting is that as pointed out by Werthmüller et al. [25] the second narrow peak is much weaker in the $\gamma n \rightarrow \eta n$ reaction than η photoproduction off the proton. So, the situation is quite opposite to the case of the first narrow bump-like structure around $W \sim 1.68$ GeV, that is to say there exists an *proton anomaly* in the case of the second narrow peak.

Mart proposed a possible finding of the narrow nucleon resonance in $K^0\Lambda$ photoproduction off the neutron [26–28], though the suggested value of the mass is lower than 1.68 GeV. Very recently, the FOREST Collaboration [29, 30] carried out the measurement of $K^0\Lambda$ photoproduction off the quasi-free neutron and the CLAS Collaboration [31, 32] have reported the data on the total and differential cross sections of $\gamma d \rightarrow K^0\Lambda(p)$. Kim et al. [33] were able to explain the experimental data on both the total and differential cross sections with the narrow nucleon resonance $N(1685)1/2^+$ included. The results of the differential cross section revealed the effects of the $N^*(1685)1/2^+$ in the forward direction near threshold.

Polyakov and Rathke [34] demonstrated based on the chiral quark-soliton model (χ QSM) [35–37] that the dipole magnetic transitions between the antidecuplet ($[\overline{10}]$) nucleon and the octet ($[8]$) nucleon has a large isospin asymmetry, i.e. the ratio becomes $\mu_{nn\overline{10}}/\mu_{pp\overline{10}} > 2$ at least. Thus, if one assumes that the narrow resonance $N^*(1685)$ belongs to the baryon antidecuplet, the large isospin asymmetry of the magnetic dipole transitions can bring about the neutron anomaly in η photoproduction off the nucleons. A more quantitative studies on the dipole magnetic transitions were carried out in Refs. [38–40] within the same framework but with the SU(3) symmetry breaking effects considered. Using also the same framework, Praszalowicz and Goeke [41] examined the masses and strong decay widths of the baryon eikosiheptaplet ($[27]$). If one assumes that the second narrow peak belongs to the baryon eikosiheptaplet, the

prediction of its mass is in qualitative agreement with the data. However, certain uncertainties were unavoidable in these mentioned previous works, so the results could not be determined unambiguously. In Refs. [44, 48], the masses of the lowest-lying baryons including the decuplet and antidecuplet were unequivocally determined by including the effects of isospin symmetry breaking arising from both the difference of the quark masses and the electromagnetic (EM) self-energies [49]. These works allowed one to determine all the relevant parameters for the vector and axial-vector properties of the baryons [50] even including those of heavy baryons [51, 52]. Thus, in the present work, we investigate both the strong and radiative decay widths of both the pronounced narrow resonances within the χ QSM, assuming that the first narrow bump-like structure or $N^*(1685)1/2^+$ belongs to the baryon antidecuplet and the second narrow peak or $N^*(1726)3/2^+$ to the baryon eikosiheptaplet. The great virtue of the present work is that we do not have any additional parameters to adjust, since all relevant dynamical parameters have been fixed in Refs. [44, 48–50]. We will demonstrate the following four significant points in this work, all of which were relevant to the existing experimental observations:

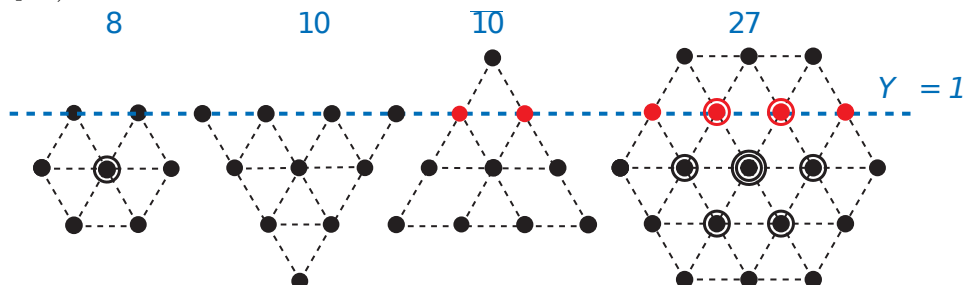
- The second narrow peak can most likely be identified as $N^*(1726)3/2^+$. The masses of those with spin 1/2 turn out to be larger than 2 GeV. The predicted mass of $N^*(1726)3/2^+$ is $M_{N_{27}} = (1719.6 \pm 7.4)$ MeV.
- Both the narrow nucleon resonances $N^*(1685)1/2^+$ and $N^*(1726)3/2^+$ can be found more clearly in the η channel than the pion channel, since the values of the strong decay widths $\Gamma_{\eta N}$ are respectively 2.6 and 31 times larger than those of $\Gamma_{\pi N}$.
- The ratio of the radiative decay widths for $N^*(1685)1/2^+$ turns out to be $\Gamma_{n_{\overline{10}}(1685)n} / \Gamma_{p_{\overline{10}}(1685)p} = 8.62$, which explains the reason for the neutron anomaly. The ratio of the radiative decay widths for $N^*(1726)3/2^+$ turns out to be $\Gamma_{p_{27}(1726)p} / \Gamma_{n_{27}(1726)n} = 3.76$, which explains the reason for the proton anomaly, though the result is not as prominent as that of $N^*(1685)1/2^+$.
- The N_{27} is more likely to be observed in decays with strangeness than $N_{\overline{10}}$.

The present paper is organized as follows: In Section II, we briefly recapitulate the general formalism of the χ QSM, focusing on the strong and radiative decays of $N^*(1685)$ and $N^*(1726)$. In Section III, we present the predicted masses of the antidecuplet and eikosiheptaplet nucleons. In Section IV, we show the results of the strong and radiative decays of $N^*(1685)$ and $N^*(1726)$ and discuss them in the context of recent experimental data. In the final Section, we summarize the present work and draw conclusions.

II. COLLECTIVE HAMILTONIAN AND WAVEFUNCTIONS OF SU(3) BARYONS

In the χ QSM, the SU(3) soliton is built from a hedgehog ansatz which requires the embedding of the SU(2) soliton into SU(3) [53]. Then the semiclassical quantization can be performed by rotating the soliton in both configuration space and flavor space simultaneously. Since the SU(2) soliton commutes with the hypercharge operator, we have only the seven zero rotational modes. Thus, the hypercharge operator does not correspond to any zero mode. It means that eight component of the generalized momenta conjugate to the right angular velocities turns out to be constrained, so that the right hypercharge becomes $Y' = N_c B / 3 = 1$, where N_c is the number of colors and B is the baryon number. The constraint on the right hypercharge is imposed by the valence quark in the χ QSM [36, 37], whereas it comes from the Wess-Zumino term in the Skyrme model [54–56]. The right hypercharge $Y' = 1$ allows the baryon representations that contain those with right hypercharge $Y' = 1$. If the number of the baryons with $Y' = 1$ is expressed as $2J + 1$, then the spin of the allowed multiplet should be equal to J (see Fig. 1).

Figure 1. Weight diagrams for the lowest-lying baryon multiplets: from the left, the baryon octet, decuplet, antidecuplet and eikosiheptaplet (**27**-plet).



Having performed the SU(3) zero-mode quantization, we can express the collective Hamiltonian as

$$H = M_{\text{cl}} + H_{\text{rot}} + H_{\text{sb}}^{\text{iso}} + H_{\text{sb}}^{\text{SU}(3)}, \quad (1)$$

where M_{cl} denotes the classical soliton mass. The $1/N_c$ rotational term, the isospin breaking one, and the SU(3) symmetry breaking one are respectively written as

$$\begin{aligned} H_{\text{rot}} &= \frac{1}{2I_1} \sum_{i=1}^3 \hat{J}_i^2 + \frac{1}{2I_2} \sum_{p=4}^7 \hat{J}_p^2, \\ H_{\text{sb}}^{\text{iso}} &= \Delta_{\text{du}} \left(\frac{\sqrt{3}}{2} \alpha D_{38}^{(8)}(A) + \beta \hat{T}_3 + \frac{1}{2} \gamma \sum_{i=1}^3 D_{3i}^{(8)}(A) \hat{J}_i \right), \\ H_{\text{sb}}^{\text{SU}(3)} &= \Delta_{\text{s}} \left(\alpha D_{88}^{(8)}(A) + \beta \hat{Y} + \frac{1}{\sqrt{3}} \gamma \sum_{i=1}^3 D_{8i}^{(8)}(A) \hat{J}_i \right) + (m_{\text{u}} + m_{\text{d}} + m_{\text{s}}) \sigma, \end{aligned} \quad (2)$$

$$(3)$$

where I_1 and I_2 stand for the moments of inertia of the soliton [36, 57]. J_i and J_p denote the generators of the SU(3) group. Δ_{du} and Δ_{s} are defined by $\Delta_{\text{du}} = m_{\text{d}} - m_{\text{u}}$ and $\Delta_{\text{s}} = m_{\text{s}} - \bar{m}$, where m_{u} , m_{d} , and m_{s} designate the current quark masses with the corresponding flavor. \bar{m} is the average current mass of the up and down quarks, $\bar{m} = (m_{\text{u}} + m_{\text{d}})/2$. We are not able to determine separately the model parameters α , β , and γ but we do not need to separate them, since we can determine all these parameters by using the masses of the baryon octet, the Ω^- mass, and that of the putative Θ^+ . σ is defined as

$$\sigma = -(\alpha + \beta) = \frac{1}{3} \frac{\Sigma_{\pi N}}{\bar{m}}, \quad (4)$$

where $\Sigma_{\pi N}$ stands for the πN sigma term. The parameters in Eq. (3) have been already determined in Ref. [44]:

$$\begin{aligned} \Delta_{\text{du}} \alpha &= -4.390 \pm 0.004, & \Delta_{\text{s}} \alpha &= -255.029 \pm 5.821, \\ \Delta_{\text{du}} \beta &= -2.411 \pm 0.001, & \Delta_{\text{s}} \beta &= -140.040 \pm 3.195, \\ \Delta_{\text{du}} \gamma &= -1.740 \pm 0.006, & \Delta_{\text{s}} \gamma &= -101.081 \pm 2.332, \end{aligned} \quad (5)$$

in units of MeV. We will use these values to calculate the masses of the $N^*(1685)$ and $N^*(1726)$. $D_{ij}^{(8)}(A)$ in Eq. (3) denotes the SU(3) Wigner D functions.

In the (p, q) representation of the SU(3) group, the sum of the generators can be expressed in terms of p and q

$$\sum_{i=1}^8 J_i^2 = \frac{1}{3} [p^2 + q^2 + p q + 3(p + q)], \quad (6)$$

which yields the eigenvalues of the rotational collective Hamiltonian H_{rot} in Eq. (2) as follows:

$$E_{(p,q),J} = \mathcal{M}_{\text{cl}} + \frac{1}{2} \left(\frac{1}{I_1} - \frac{1}{I_2} \right) J(J+1) + \frac{1}{6I_2} (p^2 + q^2 + 3(p+q) + p q) - \frac{3}{8I_2}. \quad (7)$$

Then the allowed SU(3) baryon multiplets with zero triality are obtained as

$$\begin{aligned} (p, q) = (1, 1) &\rightarrow J = 1/2 \text{ (octet)}, \\ (p, q) = (3, 0) &\rightarrow J = 3/2 \text{ (decuplet)}, \\ (p, q) = (0, 3) &\rightarrow J = 1/2 \text{ (antidecuplet)}, \\ (p, q) = (2, 2) &\rightarrow J = 1/2, J = 3/2 \text{ (eikosiheptaplet)}. \end{aligned} \quad (8)$$

Note that the eikosiheptaplet has two degenerate representations with $J = 1/2$ and $J = 3/2$. The mass splittings between the centers of the multiplets $\bar{M}_{\mathcal{R}}^J$, $(E_{(p,q)}^J)$ are determined by the moments of inertia

$$\begin{aligned} \bar{M}_{\mathbf{10}} - \bar{M}_{\mathbf{8}} &= E_{(0,3)}^{1/2} - E_{(1,1)}^{1/2} = \frac{3}{2I_2}, \\ \bar{M}_{\mathbf{27}}^{1/2} - \bar{M}_{\mathbf{8}} &= E_{(2,2)}^{1/2} - E_{(1,1)}^{1/2} = \frac{5}{2I_2}, \\ \bar{M}_{\mathbf{27}}^{3/2} - \bar{M}_{\mathbf{8}} &= E_{(2,2)}^{3/2} - E_{(1,1)}^{1/2} = \frac{3}{2I_1} + \frac{1}{I_2}, \end{aligned} \quad (9)$$

where the center mass values of the antidecuplet and eikosiheptplet are obtained as

$$\overline{M}_{\overline{10}} = 1854.9 \pm 10.0 \text{ MeV}, \quad \overline{M}_{\mathbf{27}}^{1/2} = 2324.7 \pm 16.7 \text{ MeV}, \quad \overline{M}_{\mathbf{27}}^{3/2} = 1860.4 \pm 6.7 \text{ MeV}. \quad (10)$$

The baryon wavefunctions for ta representation \mathcal{R} are written in terms of the SU(3) Wigner D functions [44, 57]:

$$\langle A | \mathcal{R}, B(Y T T_3, Y' J J_3) \rangle = \Psi_{(\mathcal{R}^*; Y' J J_3)}^{(\mathcal{R}; Y T T_3)}(A) = \sqrt{\dim(\mathcal{R})} (-)^{J_3+Y'/2} D_{(Y, T, T_3)(-Y', J, -J_3)}^{(\mathcal{R})^*}(A), \quad (11)$$

where \mathcal{R} denotes one of the allowed irreducible representations in SU(3), i.e. $\mathcal{R} = \mathbf{8}, \mathbf{10}, \overline{\mathbf{10}}, \mathbf{27}, \dots$. Y, T, T_3 are the corresponding hypercharge, isospin and its third component, respectively. As mentioned previously, the right hypercharge is constrained to be $Y' = 1$.

The presence of the SU(3) symmetry breaking term in Eq. (3) will drive a baryon state to be mixed with those from higher representations. Thus, the wavefunctions for the baryon octet, the decuplet, the antidecuplet, and the eikosiheptplet are expressed respectively as

$$\begin{aligned} |B_{\mathbf{8}}\rangle &= |\mathbf{8}_{1/2}, B\rangle + c_{\overline{\mathbf{10}}}^B |\overline{\mathbf{10}}_{1/2}, B\rangle + c_{\mathbf{27}}^B |\mathbf{27}_{1/2}, B\rangle, \\ |B_{\mathbf{10}}\rangle &= |\mathbf{10}_{3/2}, B\rangle + a_{\mathbf{27}}^B |\mathbf{27}_{3/2}, B\rangle + a_{\mathbf{35}}^B |\mathbf{35}_{3/2}, B\rangle, \\ |B_{\overline{\mathbf{10}}}\rangle &= |\overline{\mathbf{10}}_{1/2}, B\rangle + d_{\mathbf{8}}^B |\mathbf{8}_{1/2}, B\rangle + d_{\mathbf{27}}^B |\mathbf{27}_{1/2}, B\rangle + d_{\overline{\mathbf{35}}}^B |\overline{\mathbf{35}}_{1/2}, B\rangle, \\ |B_{\mathbf{27}}^{1/2}\rangle &= |\mathbf{27}_{1/2}, B\rangle + n_{\mathbf{8}}^B |\mathbf{8}_{1/2}, B\rangle + n_{\overline{\mathbf{10}}}^B |\overline{\mathbf{10}}_{1/2}, B\rangle + n_{\overline{\mathbf{35}}}^B |\overline{\mathbf{35}}_{1/2}, B\rangle + n_{\mathbf{64}}^B |\mathbf{64}_{1/2}, B\rangle, \\ |B_{\mathbf{27}}^{3/2}\rangle &= |\mathbf{27}_{3/2}, B\rangle + m_{\mathbf{10}}^B |\mathbf{10}_{3/2}, B\rangle + m_{\mathbf{35}}^B |\mathbf{35}_{3/2}, B\rangle + m_{\overline{\mathbf{35}}}^B |\overline{\mathbf{35}}_{3/2}, B\rangle + m_{\mathbf{64}}^B |\mathbf{64}_{3/2}, B\rangle, \end{aligned} \quad (12)$$

where the mixing coefficients in Eq. (12) are presented in Appendix A. Note that $|B_{\mathcal{R}}^J\rangle$ will be reduced to the pure state $|\mathcal{R}_J, B\rangle$ of Eq. (11), if one takes the limit of $m_s \rightarrow 0$.

The results of the mass splittings for the baryon decuplet and antidecuplet have been already presented and discussed in Ref. [44]. However, we recapitulate them in the present work in Tables I, II, and III given below. We use the masses of the Ω^- and Θ^+ as input together with those of the baryon octet. We could use the mass of the $N_{\overline{10}}$ as input instead of Θ^+ but it is more reasonable to choose that of Θ^+ since it is the isosinglet. By the same token, we choose the mass of Ω^- as input to determine the masses of all other members of the baryon decuplet. In addition, we also considered the contributions of the isospin symmetry breaking such that we are able to use all the masses of the baryon octet as input. There are two different contributions on the isospin symmetry breaking: the hadronic part and the electromagnetic part, both of which were included in the calculation of the mass splittings of the lowest-lying SU(3) baryons. We find that the present scheme yields robust results. In particular, we are able to reproduce the masses of the baryon decuplet without any additional parameters introduced.

Table I. Reproduced masses of the baryon octet. The experimental data of octet baryons are taken from the Particle Data Group (PDG).

Mass [MeV]	T_3	Y	Exp. [Inputs]	Numerical results
M_N	p	1/2	938.27203 \pm 0.00008	938.76 \pm 3.65
	n	-1/2	939.56536 \pm 0.00008	940.27 \pm 3.64
M_Λ	Λ	0	1115.683 \pm 0.006	1109.61 \pm 0.70
	Σ^+	1	1189.37 \pm 0.07	1188.75 \pm 0.70
M_Σ	Σ^0	0	1192.642 \pm 0.024	1190.20 \pm 0.77
	Σ^-	-1	1197.449 \pm 0.030	1195.48 \pm 0.71
M_Ξ	Ξ^0	1/2	1314.83 \pm 0.20	1319.30 \pm 3.43
	Ξ^-	-1/2	1321.31 \pm 0.13	1324.52 \pm 3.44

In Table I, we list the reproduced masses of the baryon octet. In Table II, we present the results of the decuplet masses. We find that the masses of the Σ^* and Ξ^* are remarkably in good agreement with the data within 0.5%. Table III lists the predictions of the antidecuplet masses. In fact, the existence of Θ^+ is putative and controversial. Even though it exists, it is still very difficult to measure it experimentally, because of its small decay width. For example, the DIANA Collaboration announced recently the decay width of Θ^+ to be 0.34 ± 0.10 MeV [45]. Though the existence of the baryon antidecuplet is questionable because of lack of experimental data, we hope that future experiments at the J-PARC with the kaon beam may put a period on the matter whether Θ^+ exists or not [46]. So far, the masses of the $\Sigma_{\overline{10}}$ were not observed experimentally. One can explain a possible reason as follows: Since the $\Sigma_{\overline{10}}$ has the same strangeness as usual hyperons, it is rather difficult to distinguish them from other excited hyperons within the range from 1.8 GeV to 2.0 GeV. When it comes to the $\Xi_{3/2}$, one of the corresponding multiplet

Table II. Predicted masses of the baryon decuplet. The experimental data of octet baryons are taken from the Particle Data Group (PDG).

Mass [MeV]	T_3	Y	Experiment [42]	Predictions	
Δ^{++}	3/2			1248.54 ± 3.39	
M_Δ	Δ^+	1/2	1231 – 1233	1249.36 ± 3.37	
	Δ^0	-1/2		1251.53 ± 3.38	
	Δ^-	-3/2		1255.08 ± 3.37	
	Σ^{*+}	1		1382.8 ± 0.4	1388.48 ± 0.34
M_{Σ^*}	Σ^{*0}	0	1383.7 ± 1.0	1390.66 ± 0.37	
	Σ^{*-}	-1	1387.2 ± 0.5	1394.20 ± 0.34	
	Ξ^{*0}	1/2	1531.80 ± 0.32	1529.78 ± 3.38	
$M_{\Xi^{*0}}$	Ξ^{*-}	-1/2	1535.0 ± 0.6	1533.33 ± 3.37	
	$M_{\Omega^*}^-$	Ω^-	0	-2	1672.45 ± 0.29

Table III. Predicted masses of the baryon antidecuplet.

Mass	T_3	Y	Experiment	Predictions	
M_{Θ^+}	Θ^+	0	2	1524 ± 5 [43]	Input
$M_{N_{\overline{10}}}$	$p_{\overline{10}}$	1/2	1	1686 ± 12 [11]	1688.18 ± 10.53
	$n_{\overline{10}}$	-1/2			1692.16 ± 10.53
$M_{\Sigma_{\overline{10}}}$	$\Sigma_{\overline{10}}^+$	1	0		1852.35 ± 10.00
	$\Sigma_{\overline{10}}^0$	0			1856.33 ± 10.00
	$\Sigma_{\overline{10}}^-$	-1			1858.95 ± 10.00
	$\Xi_{\overline{10}}^+$	3/2			2016.53 ± 10.53
$M_{\Xi_{3/2}}$	$\Xi_{3/2}^0$	1/2	-1		2020.51 ± 10.53
	$\Xi_{3/2}^-$	-1/2			2023.12 ± 10.53
	$\Xi_{3/2}^-$	-3/2			2024.37 ± 10.53
	$\Xi_{3/2}^-$	-3/2			2024.37 ± 10.53

has double negative charge. In fact, The finding of $\Xi_{3/2}$ was reported by the NA49 Collaboration [47], though it was not confirmed by other experiments. Moreover, the $\Xi_{3/2}$ mass observed by the NA49 Collaboration, 1.862 ± 0.002 GeV, is quite different from the predictions of the present work as shown in Table III.

On the other hand, $N_{\overline{10}}(1685)$ is experimentally found to decay exclusively into ηN , which is a unique feature in comparison with all other N^* resonances except for the $N^*(1535)$. Thus, assuming that $N_{\overline{10}}(1685)$ belongs to the baryon antidecuplet, we can systematically investigate its properties within the present framework. In the present work, we will focus on the $N_{\overline{10}}$ and N_{27} , regarding them as the pentaquark baryons. We will keep all the parameters the same as in the previous works. In the next Section, we first discuss the results of the $N_{\overline{10}}$ and N_{27} masses and then we continue to examine the radiative and strong decays of them.

III. MASSES OF THE ANTIDECUPLET AND EIKOSIHEPTAPLET NUCLEONS

The centers of mass splittings \overline{M}_{27}^J can be easily determined by the center mass of the octet baryon and the soliton moments of inertia $I_{1,2}$, since the splittings between different representations are provided with the rotational excitations:

$$\begin{aligned} \overline{M}_{27}^{1/2} &= \overline{M}_{\mathbf{8}} + \frac{5}{2I_2}, \\ \overline{M}_{27}^{3/2} &= \overline{M}_{\mathbf{8}} + \frac{3}{2I_1} + \frac{1}{I_2}, \end{aligned} \quad (13)$$

where $\overline{M}_{\mathbf{8}}$ denotes the center mass of the baryon octet derived in Ref.[44]. In order to compute the masses of the antidecuplet and eikosiheptaplet nucleons quantitatively, we need to include the EM self-energies in addition to the isospin symmetry breaking arising from the difference between the current up and down quark masses and the SU(3) symmetry breaking term given in Eq. (3). In Refs. [44, 49], the collective operator for the EM self-energies are given by

$$\mathcal{O}^{\text{EM}} = \delta^{(27)} \left(\sqrt{5} D_{\Sigma_2^0 \Lambda_{27}}^{(27)} + \sqrt{3} D_{\Sigma_1^0 \Lambda_{27}}^{(27)} + D_{\Lambda_{27} \Lambda_{27}}^{(27)} \right) + \delta^{(8)} \left(\sqrt{3} D_{\Sigma^0 \Lambda}^{(8)} + D_{\Lambda \Lambda}^{(8)} \right) + \delta^{(1)} D_{\Lambda \Lambda}^{(1)}, \quad (14)$$

where $\delta^{(n)}$ with $n = 1, 8, 27$ encodes specific dynamics of the χ QSM. We can determine $\delta^{(27)}$ and $\delta^{(8)}$ by using the empirical data estimated in Ref. [58]. $\delta^{(1)}$ can be absorbed in the center masses. Sandwiching the operator in Eq. (14) between the nucleon states, we can get the corrections of the EM self-energies to the masses of the antidecuplet and eikosiheptaplet nucleons. The explicit expressions can be found in Table VII in Appendix B. The effects of the isospin symmetry breaking arising from the current quark mass difference can be also obtained in a similar manner. See also Table VII in Appendix B for the expressions of the corrections of the the isospin symmetry breaking due to the current quark mass difference. Concerning the effects of the flavor SU(3) symmetry breaking, we compute the matrix elements of $H_{sb}^{\text{SU}(3)}$ in Eq. (3). The explicit expressions for the SU(3) symmetry breaking part can be found also in Table VII.

Table IV. Predicted values of the masses for the antidecuplet and eikosiheptaplet nucleons in units of MeV.

	States	T_3	Mass	Average
$\overline{\mathbf{10}}_{1/2}$	$N_{\overline{\mathbf{10}}}$ $p_{\overline{\mathbf{10}}}$	1/2	1688.2 ± 10.5	1690.2 ± 10.5
	$n_{\overline{\mathbf{10}}}$	-1/2	1692.2 ± 10.5	
$\mathbf{27}_{1/2}$	$N_{\mathbf{27}}$ $p_{\mathbf{27}}$	1/2	2115.7 ± 17.0	2116.6 ± 17.0
	$n_{\mathbf{27}}$	-1/2	2117.4 ± 17.0	
$\mathbf{27}_{3/2}$	$N_{\mathbf{27}}$ $p_{\mathbf{27}}$	1/2	1718.6 ± 7.4	1719.6 ± 7.4
	$n_{\mathbf{27}}$	-1/2	1720.6 ± 7.4	

In Table IV, we list the numerical results of the antidecuplet and eikosiheptaplet nucleons in units of MeV. We want to emphasize again that these values have been produced by using the parameters given in Eq. (5). The effects of isospin symmetry breaking are stronger on $N^*(1685)$ than on $N_{\mathbf{27}}$'s. In general, the EM effects ($\Delta M_{N_{\mathcal{R}}}^{\text{EM}}$) are approximately two times smaller than the current quark mass difference ($\Delta M_{N_{\mathcal{R}}}^{d-u}$). We get for the antidecuplet neutron $\Delta M_{n_{\overline{\mathbf{10}}}}^{\text{EM}} = (0.7 \pm 0.2)$ MeV and $\Delta M_{n_{\overline{\mathbf{10}}}}^{d-u} = 1.4$ MeV, and for $p_{\overline{\mathbf{10}}}$ we find $\Delta M_{p_{\overline{\mathbf{10}}}}^{\text{EM}} = (-0.4 \pm 0.2)$ MeV and $\Delta M_{p_{\overline{\mathbf{10}}}}^{d-u} = -1.4$ MeV. On the other hand, we obtain $\Delta M_{n_{\mathbf{27}}}^{\text{EM}}(J = 1/2) = (-1.0 \pm 0.3)$ MeV and $\Delta M_{n_{\mathbf{27}}}^{d-u}(J = 1/2) = 1.2$ MeV, $\Delta M_{p_{\mathbf{27}}}^{\text{EM}}(J = 1/2) = (-0.5 \pm 0.3)$ MeV, and $\Delta M_{p_{\mathbf{27}}}^{d-u}(J = 1/2) = -1.2$ MeV. So, the EM effects on $n_{\mathbf{27}}(J = 1/2)$ is canceled by the corresponding isospin symmetry breaking effects in the case of the eikosiheptaplet neutron. As a result, the isospin mass difference between the eikosiheptaplet neutron and the corresponding proton turns out to be smaller than that between $n_{\overline{\mathbf{10}}}$ and $p_{\overline{\mathbf{10}}}$.

The predicted masses of $N^*(1685)$ turn out to be slightly larger than those found in experimental data. Notably, the masses of the $N_{\mathbf{27}}(J = 3/2)$ are found to be smaller than those of $N_{\mathbf{27}}(J = 1/2)$, which was already shown in Ref. [41], though the values in Ref. [41] depend on $\Sigma_{\pi N}$. Note that in the present framework the $\Sigma_{\pi N}$ was also predicted [44]. Thus the second narrow peak observed in several experiments can be identified as an eikosiheptaplet nucleon. The predicted mass of the eikosiheptaplet neutron is (1720.6 ± 7.4) MeV. From now on, we will denote the notation $N_{\mathbf{27}}$ exclusively as the eikosiheptaplet nucleon with spin 3/2 for compactness.

IV. STRONG AND RADIATIVE DECAY WIDTHS OF $N_{\overline{\mathbf{10}}}$ AND $N_{\mathbf{27}}$

In this Section, we compute the strong and radiative decay widths of both the antidecuplet and eikosiheptaplet nucleons. The collective operators for the axial-vector and magnetic transitions [50, 59–61]

$$\hat{g}_1 = \hat{g}_1^{(0)} + \hat{g}_1^{(1)}, \quad (15)$$

$$\hat{\mu} = \hat{\mu}^{(0)} + \hat{\mu}^{(1)}, \quad (16)$$

where

$$\hat{g}_1^{(0)} = a_1 D_{\varphi 3}^{(8)} + a_2 d_{3bc} D_{\varphi b}^{(8)} \hat{J}_c + \frac{a_3}{\sqrt{3}} D_{\varphi 8}^{(8)} \hat{J}_3, \quad (17)$$

$$\hat{g}_1^{(1)} = \frac{a_4}{\sqrt{3}} d_{pq3} D_{\varphi p}^{(8)} D_{8q}^{(8)} + a_5 \left(D_{\varphi 3}^{(8)} D_{88}^{(8)} + D_{\varphi 8}^{(8)} D_{83}^{(8)} \right) + a_6 \left(D_{\varphi 3}^{(8)} D_{88}^{(8)} - D_{\varphi 8}^{(8)} D_{83}^{(8)} \right), \quad (18)$$

$$\hat{\mu}^{(0)} = w_1 D_{Q3}^{(8)} + w_2 d_{3bc} D_{Qb}^{(8)} \hat{J}_c + \frac{w_3}{\sqrt{3}} D_{Q8}^{(8)} \hat{J}_3, \quad (19)$$

$$\hat{\mu}^{(1)} = \frac{w_4}{\sqrt{3}} d_{pq3} D_{Qp}^{(8)} D_{8q}^{(8)} + w_5 \left(D_{Q3}^{(8)} D_{88}^{(8)} + D_{Q8}^{(8)} D_{83}^{(8)} \right) + w_6 \left(D_{Q3}^{(8)} D_{88}^{(8)} - D_{Q8}^{(8)} D_{83}^{(8)} \right). \quad (20)$$

$\hat{g}_1^{(0)}$ and $\hat{\mu}^{(0)}$ denote the SU(3) symmetric parts of the collective operators for the axial-vector and magnetic dipole transition, respectively. $\hat{g}_1^{(1)}$ and $\hat{\mu}^{(1)}$ represent those of the SU(3) symmetry breaking, respectively. d_{3bc} and d_{pq3} designate the SU(3) symmetric invariant tensors. The subscript index φ of $D_{\varphi 8}^{(8)}$ in the axial-vector operator means a pseudoscalar meson in the final state of a strong decay of $N_{\overline{10}}$ ($N_{\mathbf{27}}$). Q of $D_{Q8}^{(8)}$ in the magnetic dipole transition operator stands for the electric charge $Q = T_3 + Y/2$. The dynamical parameters a_i and w_i encode specific dynamics of the χ QSM. a_i were determined by using the experimental data on hyperon semileptonic decays of the baryon octet and the empirical value of the singlet axial-vector charge of the proton whereas w_i were fixed by those on the magnetic moments of the baryon octet. We refer to Ref. [50] for the details of how these parameters were determined. Thus, we take the numerical values of a_i and w_i from Ref. [50]:

$$\begin{aligned} a_1 &= -3.509 \pm 0.011, & a_2 &= 3.437 \pm 0.028, & a_3 &= 0.604 \pm 0.030, \\ a_4 &= -1.213 \pm 0.068, & a_5 &= 0.479 \pm 0.025, & a_6 &= -0.735 \pm 0.040, \end{aligned} \quad (21)$$

and

$$\begin{aligned} w_1 &= -13.515 \pm 0.010, & w_2 &= 4.147 \pm 0.933, & w_3 &= 8.544 \pm 0.861, \\ w_4 &= -3.793 \pm 0.209, & w_5 &= -4.928 \pm 0.862, & w_6 &= -2.013 \pm 0.842. \end{aligned} \quad (22)$$

We want to mention that strong decay widths of the baryon decuplet have been reproduced in very good agreement with the experimental data [61] with the numerical values of a_i in Eq. (21) employed. The magnetic moments of the baryon decuplet were also obtained to be in good agreement with the data.

Sandwiching the axial-vector transition operator between the baryon states given in Eq (12), we obtain the axial-vector transition constants $g_1^{B_i \rightarrow B_f}$. The explicit expressions for the axial-vector transition constants $g_1^{(B_i \rightarrow B_f)}$ can be found in Appendix C. Since, however, the pseudovector coupling constants, $f_{\varphi B_f B_i}$, are often used in the description of hadronic reaction, we will relate the axial-vector transition constants to them by the usual formula

$$f_{\varphi B_f B_i} = \frac{m_{\varphi}}{f_{\varphi}} g_1^{B_i \rightarrow B_f}, \quad (23)$$

where m_{φ} and f_{φ} denote the mass and the decay constant of a pseudoscalar meson involved in a strong decay, respectively. To obtain the pseudovector coupling constants, we have used the following numerical values of the pseudoscalar meson masses and decay constants [42, 62]

$$\begin{aligned} f_{\pi} &= 92.4 \text{ MeV}, & m_{\pi} &= 137.57 \text{ MeV}, \\ f_K &= 113.0 \text{ MeV}, & m_K &= 493.7 \text{ MeV}, \\ f_{\eta} &= 94.0 \text{ MeV}, & m_{\eta} &= 547.9 \text{ MeV}. \end{aligned} \quad (24)$$

Using the results of Eq. (23), we can easily derive the expression for the strong decays as follows

$$\Gamma_{B_i \rightarrow \varphi + B_f} = \frac{|\mathbf{P}_{\varphi}|^3}{6\pi m_{\varphi}^2} \frac{M_f}{M_i} (f_{\varphi B_f B_i})^2, \quad (25)$$

where \mathbf{P}_{φ} is the momentum of the outgoing pseudoscalar meson φ . Note that the strong coupling constants $f_{\varphi B_f B_i}$ include the factors coming from the average and summation over the initial and final spin and isospin states, respectively.

Since we are mainly interested in the decays of $N^*(1685)1/2^+$ and $N^*(1726)3/2^+$ into ηN , we need to derive the $\eta N N_{\overline{10}}(N_{\mathbf{27}})$ coupling constants, which means that we need to extract them from the singlet η_0 and octet η_8 coupling constants. Introducing the mixing angle, we can get $f_{\eta B_f B_i}$ and $f_{\eta' B_f B_i}$ as follows

$$\begin{aligned} f_{\eta B_f B_i} &= \cos\theta_p f_{\eta_8 B_f B_i} - \sin\theta_p f_{\eta_0 B_f B_i}, \\ f_{\eta' B_f B_i} &= \sin\theta_p f_{\eta_8 B_f B_i} + \cos\theta_p f_{\eta_0 B_f B_i}, \end{aligned} \quad (26)$$

where the mixing angle $\theta_p = -15.5^\circ$ is taken from Ref. [63].

The numerical results of the pseudovector coupling constants and the strong decay widths for the $N^*(1685)1/2^+$ and $N^*(1726)3/2^+$ are listed in Table V. As shown from Table V, the leading-order contributions are suppressed, so that the effects of SU(3) symmetry breaking become very important. This can be understood by examining the leading-order expressions of the axial-vector coupling constants for the vertices $N_{\overline{10}} \rightarrow \varphi + N$ and $N_{\mathbf{27}} \rightarrow \varphi + N$ in

Table V. Numerical results of the pseudovector coupling constants and strong decay widths of the antidecuplet nucleon and eikosiheptaplet nucleon with spin 3/2.

\mathcal{R}_J	$B_i \rightarrow \varphi + B_f$	$f_{\varphi B_f B_i}^{(0)}$	$f_{\varphi B_f B_i}^{(\text{tot})}$	$\Gamma_{\varphi B_f B_i}^{(0)}$ [MeV]	$\Gamma_{\varphi B_f B_i}^{(\text{tot})}$ [MeV]	$\Gamma_{\varphi B_f B_i}^{(\text{Full})}$ [MeV]
$\overline{10}_{1/2}$	$N_{\overline{10}} \rightarrow \pi + N$	-0.04 ± 0.01	-0.17 ± 0.01	0.42 ± 0.12	8.34 ± 1.03	
	$N_{\overline{10}} \rightarrow \eta + N$	0.96 ± 0.11	1.95 ± 0.20	5.37 ± 1.31	22.09 ± 4.89	30.5 ± 5.0
	$N_{\overline{10}} \rightarrow K + \Lambda$	-0.11 ± 0.02	-0.16 ± 0.02	0.02 ± 0.01	0.05 ± 0.02	
	$N_{\overline{10}} \rightarrow K + \Sigma$	-0.11 ± 0.02	0.055 ± 0.024	0.0001 ± 0.0008	~ 0.00003	
$27_{3/2}$	$N_{27} \rightarrow \pi + N$	-0.11 ± 0.01	0.04 ± 0.01	4.2 ± 0.1	0.6 ± 0.1	
	$N_{27} \rightarrow \eta + N$	0.43 ± 0.18	1.61 ± 0.27	1.3 ± 1.1	18.7 ± 6.2	22.2 ± 6.2
	$N_{27} \rightarrow K + \Lambda$	-1.01 ± 0.02	-0.93 ± 0.02	3.2 ± 0.3	2.7 ± 0.3	
	$N_{27} \rightarrow K + \Sigma$	0.34 ± 0.01	0.61 ± 0.02	0.06 ± 0.02	0.19 ± 0.07	

Eqs. (C1)-(C8). The expressions for $g_1^{(0)}[N_{\overline{10}} \rightarrow \varphi + N]$ are all proportional to $a_1 + a_2 + a_3/2$. As given in Eq. (21), the values of a_1 and a_2 are almost the same but the signs are different each other. On the other hand, that of a_3 is rather small. Consequently, the numerical results of $g_1^{(0)}[N_{\overline{10}} \rightarrow \varphi + N]$ turn out to be very small. The formulas for $g_1^{(0)}[N_{27} \rightarrow \varphi + N]$ are similarly proportional to $a_1 + a_2/2$, which also brings about the suppression of the leading-order contribution to the axial-vector transition coupling constants of N_{27} . Thus, the contributions of the SU(3) symmetry breaking come into play of leading roles. We want to emphasize that, however, the situation is opposite when it comes to the case of the $B_{10} \rightarrow B_8$ transitions. The leading-order expressions for $g_1^{(0)}[B_{10} \rightarrow \varphi + B_8]$ are all proportional to $a_1 - a_2/2$, which causes indeed the leading-order contributions to be the most dominant ones.

The results presented in Table V have important physical implications. The strong decay widths of both $N_{\overline{10}} \rightarrow \eta + N$ and $N_{27} \rightarrow \eta + N$ are much larger than those of $N_{\overline{10}} \rightarrow \pi + N$ and $N_{27} \rightarrow \pi + N$, respectively: the value of $\Gamma[N_{\overline{10}} \rightarrow \eta + N]$ is approximately 2.6 times larger than that of $\Gamma[N_{\overline{10}} \rightarrow \pi + N]$ and that of $\Gamma[N_{27} \rightarrow \eta + N]$ is even 31 times larger than that of $\Gamma[N_{27} \rightarrow \pi + N]$. This explains why both the narrow resonances $N^*(1685)$ and $N^*(1726)$ are more likely to be observed in η photoproduction than in $\gamma + N \rightarrow \pi + N$. The full decay widths of $N_{\overline{10}}$ and N_{27} are obtained respectively as (30.5 ± 5.0) MeV and (22.2 ± 6.2) MeV, which are indeed much narrower than usual excited nucleon resonances. In particular, the strong decay width of $N^*(1685)$ is in remarkable agreement with the experimental data on the corresponding intrinsic width that was estimated to be (30 ± 15) MeV [1, 4–6]. Note that the strong decay width of $N^*(1726)$ is predicted to be even narrower than that of $N^*(1685)$. However, there is one caveat. The present work shows relatively larger value of $\Gamma[N_{\overline{10}} \rightarrow \pi + N]$, though it is still quite smaller than that of $\Gamma[N_{\overline{10}} \rightarrow \eta + N]$. As pointed out by Goeke et al. [64], the mixing of the $N_{\overline{10}}$ with the Roper resonance provides a crucial explanation of why the $N_{\overline{10}}$ was not seen in the πN scattering data. Thus, the inclusion of the mixing with $N(1440)$ will further decrease the value of $\Gamma[N_{\overline{10}} \rightarrow \pi + N]$. However, in order to investigate the effects of this mixing, one needs to construct first a formalism of describing the spectra of excited baryons within the same framework as the present one. We leave it as a future work.

It is also interesting to look into the decay modes of both $N_{\overline{10}}$ and N_{27} with strangeness. As displayed in Table V, the decay of $N_{\overline{10}} \rightarrow K + \Sigma$ is almost forbidden, because the mass of $N_{\overline{10}}$ is smaller than the threshold of the $K\Sigma$ production. The decay of $N_{\overline{10}} \rightarrow K + \Lambda^0$ is allowed but the magnitude of the corresponding decay width is rather tiny. However, recent experiments on $K\Lambda^0$ photoproduction off the quasi-free neutron [29–32] provide some hint on the existence of the narrow nucleon resonance [33]. In contrast, the eikosiheptaplet nucleon can decay into K and Σ , though the partial decay width is rather small. However, the width for the $N_{27} \rightarrow K + \Lambda$ is about (2.7 ± 0.3) MeV, which might be detectable experimentally.

As mentioned in Introduction, the magnetic dipole transitions of the $N_{\overline{10}}$ have been investigated qualitatively in previous works [34, 38] in which a theoretical ambiguity was unavoidable because the baryon wavefunctions could not be fixed when the effects of SU(3) symmetry breaking were included. This uncertainty led to the fact that the magnetic transition moments of $N_{\overline{10}}$ are proportional to $\Sigma_{\pi N}$. Unfortunately, the leading-order contributions to $\mu_{NN_{\overline{10}}}$ were very sensitive to the change of the $\Sigma_{\pi N}$ value, so that a precise prediction was not possible in Ref. [38]. However, the present work does not have such an ambiguity anymore. In Table VI, we list the numerical results of the magnetic transition moments of both $N_{\overline{10}}$ and N_{27} . As pointed out by Refs. [34, 38], the leading-order contributions to the magnetic transition moments of $N_{\overline{10}}$ are proportional to $Q - 1$, where Q denotes the corresponding charge of $N_{\overline{10}}$. Thus, $\mu[p_{\overline{10}} \rightarrow \gamma + p]$ exactly vanishes in the leading order whereas $\mu[n_{\overline{10}} \rightarrow \gamma + n]$ has a finite value. The situation is the other way around in the case of N_{27} : those of N_{27} are proportional to $Q + 1$, so that the leading-order

Table VI. Magnetic transition moments in units of the nuclear magneton (μ_N) and radiative decay widths of the antidecuplet and eikosiheptaplet nucleons in units of keV.

$N_{\overline{10}} \rightarrow \gamma + N$	$\mu_{N_{\overline{10}}N}^{(0)}$	$\mu_{N_{\overline{10}}N}^{(\text{tot})}$	$\Gamma_{N_{\overline{10}}N\gamma}^{(\text{tot})}$ [keV]
$p_{\overline{10}} \rightarrow \gamma + p$	0	0.15 ± 0.04	18.78 ± 0.52
$n_{\overline{10}} \rightarrow \gamma + n$	-0.38 ± 0.08	-0.44 ± 0.09	161.83 ± 64.72
$N_{27} \rightarrow \gamma + N$	$\mu_{27}^{(0)}$	$\mu_{27}^{(\text{tot})}$	$\Gamma_{\gamma N_{27}N}^{(\text{tot})}$ [MeV]
$p_{27} \rightarrow \gamma + p$	-0.93 ± 0.04	-0.75 ± 0.05	1.43 ± 0.19
$n_{27} \rightarrow \gamma + n$	-0.46 ± 0.02	-0.38 ± 0.02	0.38 ± 0.04

value of $\mu[p_{27} \rightarrow \gamma + p]$ turns out to be larger than that of $\mu[n_{27} \rightarrow \gamma + n]$, which is opposite to the case of $N_{\overline{10}}$.

The expressions of the magnetic transition moments for the $N_{\overline{10}}$ and N_{27} are very similar to those of the axial-vector transitions. Namely, the leading-order contributions to $\mu[N_{\overline{10}} \rightarrow \gamma + N]$ are proportional to $w_1 + w_2 + w_3/2$ whereas $\mu[N_{27} \rightarrow \gamma + N]$ is in proportion to $w_1 + w_2/2$. It explains again the reason why the magnetic transition moments of $n_{\overline{10}}$ and N_{27} are rather small in leading order. The contributions of the SU(3) symmetry breaking become the leading one to $\mu[p_{\overline{10}} \rightarrow \gamma + p]$. In the case of $\mu[n_{\overline{10}} \rightarrow \gamma + n]$, the effects of the SU(3) symmetry breaking contribute to $\mu[N_{\overline{10}} \rightarrow \gamma + N]$ approximately by 25% and to $\mu[N_{27} \rightarrow \gamma + N]$ by about 20%.

By the reason explained above, the radiative decay width of the antidecuplet neutron turns out to be much larger than that of the antidecuplet proton. Their ratio can be explicitly obtained as

$$\frac{\Gamma_{\gamma}[n_{\overline{10}} \rightarrow n]}{\Gamma_{\gamma}[p_{\overline{10}} \rightarrow p]} = 8.62 \pm 3.45. \quad (27)$$

Thus, the neutron anomaly can be explained by this ratio, as already pointed out by Refs. [34, 38]. However, when it comes to the radiative decays of the eikosiheptaplet nucleons, p_{27} has a larger radiative decay width than n_{27} does. Thus, their ratio is obtained as

$$\frac{\Gamma_{\gamma}[p_{27} \rightarrow p]}{\Gamma_{\gamma}[n_{27} \rightarrow n]} = 3.76 \pm 0.64. \quad (28)$$

It indicates that the eikosiheptaplet nucleon is more likely to be found in η photoproduction off the proton. It is of great interest if we have a proton anomaly in finding N_{27} though it is not as prominent as the neutron anomaly in $N_{\overline{10}}$.

V. SUMMARY AND CONCLUSIONS

In the present work, we have investigate the strong and radiative decay widths of the antidecuplet and eikosiheptaplet nucleons in addition to their masses, based on the SU(3) chiral quark-soliton model. All the relevant parameters for the strong and radiative decay widths have been already fixed in the baryon octet sector, so that we do not have any additional parameter to obtain the numerical results of the strong and radiative decay widths. From the present study, we come to the following conclusions:

- The second narrow peak found in Refs. [23–25] can be identified as a member of the eikosiheptaplet with spin 3/2 [41]. Thus, the quantum numbers of this narrow nucleon resonance will be given as spin 3/2 and negative parity, i.e. $N^*(1726)3/2^+$. Other members of the eikosiheptaplet with spin 1/2 have rather large masses, i.e. $M_{N_{27}(J=1/2)} > 2 \text{ GeV}$. Thus, we did not discuss them in this work. We have predicted the mass of $N^*(1726)3/2^+$ to be $M_{N_{27}} = (1719.6 \pm 7.4) \text{ MeV}$.
- The partial decay width $\Gamma_{N_{\overline{10}} \rightarrow \eta N}$ of the antidecuplet nucleon is at least three times larger than $\Gamma_{N_{\overline{10}} \rightarrow \pi N}$. $\Gamma_{N_{27} \rightarrow \eta N}$ is even 31 times larger than $\Gamma_{N_{27} \rightarrow \pi N}$. Note, however, that Gridnev et al. [24] have seen both the narrow resonant structures from the analysis of πp elastic scattering. The present results imply that the narrow nucleon resonance $N^*(1726)3/2^+$ may be found in hadronic or photonic processes with the η meson involved.
- We found the ratio of the radiative decay widths for $N^*(1685)1/2^+$ $\Gamma_{n_{\overline{10}}(1685)n} / \Gamma_{p_{\overline{10}}(1685)p} = 8.62$. This explains the reason for the neutron anomaly as already pointed out in Refs. [34, 38]. Note that $\Gamma_{p_{\overline{10}}(1685)p}$ vanishes in the limit of SU(3) symmetry. Thus, the contribution only arises from the effects of the SU(3) symmetry breaking. It leads to the large ratio of $\Gamma_{n_{\overline{10}}(1685)n} / \Gamma_{p_{\overline{10}}(1685)p}$.

- On the other hand, the ratio of the radiative decay widths for $N^*(1726)3/2^+$ was found to be $\Gamma_{p_{27}(1726)p}/\Gamma_{n_{27}(1726)n} = 3.76$, which is opposite to the case of $N_{\overline{10}}$. Though the size of this ratio is not as noticeable as that for $N_{\overline{10}}$, the eikosiheptaplet proton is more likely to be observed in comparison with the corresponding neutron. If it is experimentally true, we can call it *proton anomaly*.
- Last but not least, it is of great interest to examine the decay modes of the antidecuplet and eikosiheptaplet nucleons with strangeness. As expected, $N_{\overline{10}}$ does not decay into K and Σ on account of the fact that the corresponding threshold energy is higher than the mass of $N_{\overline{10}}$. The decay width for $N_{\overline{10}} \rightarrow K + \Lambda$ turns out to be very small. In contrast to the antidecuplet nucleons, N_{27} is allowed to decay into K and Σ , though its magnitude is rather small. The decay width for $N_{27} \rightarrow K + \Lambda$ is (2.7 ± 0.3) MeV, which might be observed in $K\Lambda^0$ photoproduction off the proton.

ACKNOWLEDGMENT

H.-Ch. K is grateful to A. Hosaka, T. Maruyama, M. Oka for useful discussions. He wants to express his gratitude to the members of the Advanced Science Research Center, Japan Atomic Energy Agency, where part of the present work was done. Gh.-S. Y is also grateful to H.D. Son for valuable discussions. The present work was supported by Basic Science Research Program through the National Research Foundation of Korea funded by the Ministry of Education, Science and Technology (No. NRF-2019R1A2C1010443 (Gh.-S. Y.) and 2018R1A5A1025563 (H.-Ch.K.)).

Appendix A: Mixing coefficients in Eq. (12)

In this Appendix, we present the explicit expressions for the mixing coefficients in Eq. (12):

$$c_{\overline{10}}^B = -\frac{1}{3}I_2\Delta_s \left(\alpha + \frac{1}{2}\gamma \right) \begin{pmatrix} \overline{10} & \mathbf{8} & \mathbf{8} \\ B & 0,0,0 & B \end{pmatrix}, \quad c_{27}^B = \frac{3}{5\sqrt{5}}I_2\Delta_s \left(\alpha - \frac{1}{6}\gamma \right) \begin{pmatrix} \mathbf{27} & \mathbf{8} & \mathbf{8} \\ B & 0,0,0 & B \end{pmatrix}, \quad (\text{A1})$$

$$a_{27}^B = -\frac{3}{4}I_2\Delta_s \left(\alpha + \frac{5}{6}\gamma \right) \begin{pmatrix} \mathbf{27} & \mathbf{8} & \mathbf{10} \\ B & 0,0,0 & B \end{pmatrix}, \quad a_{35}^B = \frac{5}{12\sqrt{5}}I_2\Delta_s \left(\alpha - \frac{1}{2}\gamma \right) \begin{pmatrix} \mathbf{35} & \mathbf{8} & \mathbf{10} \\ B & 0,0,0 & B \end{pmatrix}, \quad (\text{A2})$$

$$d_{\mathbf{8}}^B = \frac{2}{3\sqrt{5}}I_2\Delta_s \left(\alpha + \frac{1}{2}\gamma \right) \begin{pmatrix} \mathbf{8} & \mathbf{8} & \overline{\mathbf{10}} \\ B & 0,0,0 & B \end{pmatrix}, \quad d_{27}^B = \frac{3}{4\sqrt{5}}I_2\Delta_s \left(\alpha - \frac{7}{6}\gamma \right) \begin{pmatrix} \mathbf{27} & \mathbf{8} & \overline{\mathbf{10}} \\ B & 0,0,0 & B \end{pmatrix},$$

$$d_{\overline{35}}^B = \frac{1}{4}I_2\Delta_s \left(\alpha + \frac{1}{6}\gamma \right) \begin{pmatrix} \overline{\mathbf{35}} & \mathbf{8} & \overline{\mathbf{10}} \\ B & 0,0,0 & B \end{pmatrix}, \quad (\text{A3})$$

$$n_{\mathbf{8}}^B = \frac{4}{5\sqrt{30}}I_2\Delta_s \left(\alpha - \frac{1}{6}\gamma \right) \begin{pmatrix} \mathbf{8} & \mathbf{8} & \mathbf{27} \\ B & 0,0,0 & B \end{pmatrix}, \quad n_{\overline{10}}^B = \frac{1}{2\sqrt{6}}I_2\Delta_s \left(\alpha - \frac{7}{6}\gamma \right) \begin{pmatrix} \overline{\mathbf{10}} & \mathbf{8} & \mathbf{27} \\ B & 0,0,0 & B \end{pmatrix},$$

$$n_{\overline{35}}^B = -\frac{5}{8\sqrt{15}}I_2\Delta_s \left(\alpha + \frac{5}{6}\gamma \right) \begin{pmatrix} \overline{\mathbf{35}} & \mathbf{8} & \mathbf{27} \\ B & 0,0,0 & B \end{pmatrix}, \quad n_{64}^B = \frac{20}{7\sqrt{210}}I_2\Delta_s \left(\alpha - \frac{1}{6}\gamma \right) \begin{pmatrix} \mathbf{64} & \mathbf{8} & \mathbf{27} \\ B & 0,0,0 & B \end{pmatrix}, \quad (\text{A4})$$

$$m_{\overline{10}}^B = \frac{5}{2\sqrt{30}}I_2\Delta_s \left(\alpha + \frac{5}{6}\gamma \right) \begin{pmatrix} \mathbf{10} & \mathbf{8} & \mathbf{27} \\ B & 0,0,0 & B \end{pmatrix}, \quad m_{35}^B = \frac{5}{8\sqrt{15}}I_2\Delta_s \left(\alpha - \frac{7}{6}\gamma \right) \begin{pmatrix} \mathbf{35} & \mathbf{8} & \mathbf{27} \\ B & 0,0,0 & B \end{pmatrix},$$

$$m_{\overline{35}}^B = -\frac{1}{2\sqrt{3}}I_2\Delta_s \left(\alpha + \frac{5}{6}\gamma \right) \begin{pmatrix} \overline{\mathbf{35}} & \mathbf{8} & \mathbf{27} \\ B & 0,0,0 & B \end{pmatrix}, \quad m_{64}^B = \frac{10}{7\sqrt{105}}I_2\Delta_s \left(\alpha - \frac{1}{6}\gamma \right) \begin{pmatrix} \mathbf{64} & \mathbf{8} & \mathbf{27} \\ B & 0,0,0 & B \end{pmatrix}. \quad (\text{A5})$$

Appendix B: Expressions for the masses of the antidecuplet and eikosiheptaplet nucleons

In Table VII, we tabulate each contribution to the masses of the eikosiheptaplet nucleons.

Table VII. Expressions for the masses for the eikosiheptaplet nucleons

States	T_3	EM	Isospin	$SU_f(3)$
$\mathbf{27}_{1/2}$	$N_{\mathbf{27}}$	$p_{\mathbf{27}}$	$1/2 \frac{33}{280} \left(\delta^{(8)} + \frac{6}{11} \delta^{(27)} \right) - \frac{71}{1120} \Delta_{\text{du}} \left(\alpha - \frac{560}{71} \beta + \frac{233}{142} \gamma \right)$	$\frac{137}{560} \Delta_s \left(\alpha + \frac{560}{137} \beta + \frac{71}{274} \gamma \right)$
	$n_{\mathbf{27}}$	$-1/2 \frac{13}{35} \left(\delta^{(8)} + \frac{41}{156} \delta^{(27)} \right)$	$\frac{71}{1120} \Delta_{\text{du}} \left(\alpha - \frac{560}{71} \beta + \frac{233}{142} \gamma \right)$	
$\mathbf{27}_{3/2}$	$N_{\mathbf{27}}$	$p_{\mathbf{27}}$	$1/2 \frac{3}{14} \left(\delta^{(8)} - \frac{1}{4} \delta^{(27)} \right) - \frac{5}{56} \Delta_{\text{du}} \left(\alpha + \frac{28}{5} \beta - \frac{5}{2} \gamma \right)$	$\frac{1}{28} \Delta_s \left(\alpha + 28\beta - \frac{5}{2} \gamma \right)$
	$n_{\mathbf{27}}$	$-1/2 - \frac{1}{7} \left(\delta^{(8)} + \frac{19}{24} \delta^{(27)} \right)$	$-\frac{5}{56} \Delta_{\text{du}} \left(\alpha + \frac{28}{5} \beta - \frac{5}{2} \gamma \right)$	

Appendix C: Expressions for the axial-vector transition constants

Expressions of axial-vector coupling constants of the baryon antidecuplet $N_{\overline{\mathbf{10}}}$ to the baryon octet are given below. $g_1^{(0)}$ denote the leading-order contributions to the axial-vector transition constants. Note, however, that it contains the rotational $1/N_c$ corrections. We will not decompose them in the present work and call it generically the leading-order terms. $g_1^{(\text{op})}$ represent the contributions of the $SU(3)$ symmetry breaking arising from the linear m_s expansion given in Eq. (15). $g_1^{(\text{wf})}$ stand for those from the baryon wavefunctions that also contains the linear m_s .

$$\begin{aligned}
g_1^{(0)} [N_{\overline{\mathbf{10}}} \rightarrow \pi + N] &= -\frac{1}{6\sqrt{5}} \left(a_1 + a_2 + \frac{1}{2} a_3 \right), \\
g_1^{(\text{op})} [N_{\overline{\mathbf{10}}} \rightarrow \pi + N] &= -\frac{1}{54\sqrt{5}} (a_4 + 6a_5 + 9a_6), \\
g_1^{(\text{wf})} [N_{\overline{\mathbf{10}}} \rightarrow \pi + N] &= -\frac{5}{24\sqrt{5}} \left(a_1 + \frac{5}{2} a_2 - \frac{1}{2} a_3 \right) c_{\overline{\mathbf{10}}} - \frac{49}{72\sqrt{5}} \left(a_1 - \frac{11}{14} a_2 - \frac{3}{14} a_3 \right) c_{\mathbf{27}} \\
&\quad - \frac{7}{6\sqrt{5}} \left(a_1 - \frac{1}{2} a_2 - \frac{1}{14} a_3 \right) d_{\mathbf{8}} - \frac{1}{90\sqrt{5}} \left(a_1 + 2a_2 - \frac{3}{2} a_3 \right) d_{\mathbf{27}}, \tag{C1}
\end{aligned}$$

$$\begin{aligned}
g_1^{(0)} [N_{\overline{\mathbf{10}}} \rightarrow \eta + N] &= \frac{1}{2\sqrt{15}} \left(a_1 + a_2 + \frac{1}{2} a_3 \right), \\
g_1^{(\text{op})} [N_{\overline{\mathbf{10}}} \rightarrow \eta + N] &= -\frac{1}{6\sqrt{15}} a_4, \\
g_1^{(\text{wf})} [N_{\overline{\mathbf{10}}} \rightarrow \eta + N] &= 0, \tag{C2}
\end{aligned}$$

$$\begin{aligned}
g_1^{(0)} [N_{\overline{\mathbf{10}}} \rightarrow K + \Lambda] &= -\frac{1}{2\sqrt{15}} \left(a_1 + a_2 + \frac{1}{2} a_3 \right), \\
g_1^{(\text{op})} [N_{\overline{\mathbf{10}}} \rightarrow K + \Lambda] &= \frac{1}{12\sqrt{15}} (a_4 + 3a_6), \\
g_1^{(\text{wf})} [N_{\overline{\mathbf{10}}} \rightarrow K + \Lambda] &= \frac{7}{4\sqrt{15}} \left(a_1 - \frac{11}{14} a_2 - \frac{3}{14} a_3 \right) c_{\mathbf{27}} + \frac{2}{\sqrt{15}} \left(a_1 - \frac{1}{2} a_2 - \frac{1}{4} a_3 \right) d_{\mathbf{8}} \\
&\quad - \frac{1}{10\sqrt{15}} \left(a_1 + 2a_2 - \frac{3}{2} a_3 \right) d_{\mathbf{27}}, \tag{C3}
\end{aligned}$$

$$\begin{aligned}
g_1^{(0)} [N_{\overline{\mathbf{10}}} \rightarrow K + \Sigma] &= -\frac{1}{6\sqrt{5}} \left(a_1 + a_2 + \frac{1}{2} a_3 \right), \\
g_1^{(\text{op})} [N_{\overline{\mathbf{10}}} \rightarrow K + \Sigma] &= -\frac{1}{108\sqrt{5}} (a_4 - 12a_5 + 9a_6),
\end{aligned}$$

$$\begin{aligned}
g_1^{(\text{wf})} [N_{\overline{\mathbf{10}}} \rightarrow K + \Sigma] &= -\frac{5}{12\sqrt{5}} \left(a_1 + \frac{5}{2}a_2 - \frac{1}{2}a_3 \right) c_{\overline{\mathbf{10}}} + \frac{7}{18\sqrt{5}} \left(a_1 - \frac{11}{14}a_2 - \frac{3}{14}a_3 \right) c_{\mathbf{27}} \\
&\quad + \frac{1}{3\sqrt{5}} \left(a_1 - \frac{1}{2}a_2 + a_3 \right) d_{\mathbf{8}} + \frac{1}{90\sqrt{5}} \left(a_1 + 2a_2 - \frac{3}{2}a_3 \right) d_{\mathbf{27}}.
\end{aligned} \tag{C4}$$

The following are the expressions of the axial-vector coupling constants of the baryon eikosiheptplet $N_{\mathbf{27}}$ ($J = 3/2$) to the baryon octet:

$$\begin{aligned}
g_1^{(0)} [N_{\mathbf{27}} \rightarrow \pi + N] &= \frac{2}{9\sqrt{30}} \left(a_1 + \frac{1}{2}a_2 \right), \\
g_1^{(\text{op})} [N_{\mathbf{27}} \rightarrow \pi + N] &= \frac{2}{63\sqrt{30}} \left(a_4 + 4a_5 - \frac{7}{2}a_6 \right), \\
g_1^{(\text{wf})} [N_{\mathbf{27}} \rightarrow \pi + N] &= -\frac{35}{18\sqrt{30}} (a_1 - a_2) c_{\overline{\mathbf{10}}} + \frac{191}{14\sqrt{30}} \left(a_1 - \frac{8}{19}a_2 \right) c_{\mathbf{27}},
\end{aligned} \tag{C5}$$

$$\begin{aligned}
g_1^{(0)} [N_{\mathbf{27}} \rightarrow \eta + N] &= \frac{2}{3\sqrt{10}} \left(a_1 + \frac{1}{2}a_2 \right), \\
g_1^{(\text{op})} [N_{\mathbf{27}} \rightarrow \eta + N] &= -\frac{5}{21\sqrt{10}} \left(a_4 - \frac{1}{5}a_5 \right), \\
g_1^{(\text{wf})} [N_{\mathbf{27}} \rightarrow \eta + N] &= 0,
\end{aligned} \tag{C6}$$

$$\begin{aligned}
g_1^{(0)} [N_{\mathbf{27}} \rightarrow K + \Lambda] &= \frac{2}{3\sqrt{10}} \left(a_1 + \frac{1}{2}a_2 \right), \\
g_1^{(\text{op})} [N_{\mathbf{27}} \rightarrow K + \Lambda] &= -\frac{1}{14\sqrt{10}} \left(a_4 + \frac{5}{3}a_5 - \frac{7}{3}a_6 \right), \\
g_1^{(\text{wf})} [N_{\mathbf{27}} \rightarrow K + \Lambda] &= -\frac{3}{7\sqrt{10}} \left(a_1 - \frac{16}{3}a_2 \right) c_{\mathbf{27}},
\end{aligned} \tag{C7}$$

$$\begin{aligned}
g_1^{(0)} [N_{\mathbf{27}} \rightarrow K + \Sigma] &= -\frac{2}{9\sqrt{30}} \left(a_1 + \frac{1}{2}a_2 \right), \\
g_1^{(\text{op})} [N_{\mathbf{27}} \rightarrow K + \Sigma] &= -\frac{11}{126\sqrt{30}} \left(a_4 - \frac{47}{11}a_5 + \frac{49}{11}a_6 \right), \\
g_1^{(\text{wf})} [N_{\mathbf{27}} \rightarrow K + \Sigma] &= -\frac{5}{9\sqrt{30}} (a_1 - a_2) c_{\overline{\mathbf{10}}} + \frac{6}{7\sqrt{30}} \left(a_1 + \frac{22}{9}a_2 \right) c_{\mathbf{27}}.
\end{aligned} \tag{C8}$$

Appendix D: Expressions for the dipole magnetic transition moments

Expressions of axial-vector coupling constants of the baryon antidecuplet $N_{\overline{\mathbf{10}}}$ to the baryon octet are given below (see also Ref. [38]). $\mu_{NN_{\overline{\mathbf{10}}}}^{(0)}$ denote the leading-order contributions to the axial-vector transition constants. Note, however, that it contains the rotational $1/N_c$ corrections. We will not decompose them in the present work and call it generically the leading-order terms. $\mu_{NN_{\overline{\mathbf{10}}}}^{(\text{op})}$ represent the contributions of the SU(3) symmetry breaking arising from the linear m_s expansion given in Eq. (16). $\mu_{NN_{\overline{\mathbf{10}}}}^{(\text{wf})}$ stand for those from the baryon wavefunctions that also contains the linear m_s . Expressions of transition magnetic moments of the baryon antidecuplet $N_{\overline{\mathbf{10}}}$ to N and those of the

baryon eikosiheptaplet N_{27} ($J = 3/2$):

$$\begin{aligned}
\mu_{NN_{\overline{10}}}^{(0)} &= -\frac{1}{6\sqrt{5}}(Q-1)\left(w_1 + w_2 + \frac{1}{2}w_3\right), \\
\mu_{NN_{\overline{10}}}^{(\text{op})} &= -\frac{1}{54\sqrt{5}}(Q+1)w_4 - \frac{1}{18\sqrt{5}}(2Q-1)\left(w_5 + \frac{3}{2}w_6\right), \\
\mu_{NN_{\overline{10}}}^{(\text{wf})} &= -\frac{5}{24\sqrt{5}}c_{\overline{10}}Q\left(w_1 + \frac{5}{2}w_2 - \frac{1}{2}w_3\right) - \frac{49}{72\sqrt{5}}c_{27}(7Q-2)\left(w_1 - \frac{11}{14}w_2 - \frac{3}{14}w_3\right) \\
&\quad + \frac{1}{12\sqrt{5}}d_8\left[2(3-7Q)\left(w_1 - \frac{1}{2}w_2\right) + (Q+1)w_3\right] \\
&\quad - \frac{1}{90\sqrt{5}}d_{27}(Q+1)\left(w_1 + 2w_2 - \frac{3}{2}w_3\right).
\end{aligned} \tag{D1}$$

The following are the expressions of the magnetic transition moments of the baryon eikosiheptaplet N_{27} ($J = 3/2$) to the baryon octet:

$$\begin{aligned}
\mu_{NN_{27}}^{(0)} &= \frac{2}{9\sqrt{30}}(Q+1)\left(w_1 + \frac{1}{2}w_2\right), \\
\mu_{NN_{27}}^{(\text{op})} &= \frac{1}{126\sqrt{30}}(4Q-17)\left(w_4 - \frac{11}{13}w_5 + \frac{7}{13}w_6\right), \\
\mu_{NN_{27}}^{(\text{wf})} &= -\frac{35}{18\sqrt{30}}c_{\overline{10}}(7Q-2)(w_1 - w_2) + \frac{1}{14\sqrt{30}}c_{27}[(19Q-16)w_1 - 8(Q+1)w_2].
\end{aligned} \tag{D2}$$

-
- [1] V. Kuznetsov *et al.* [GRAAL Collaboration], Phys. Lett. B **647**, 23 (2007).
[2] F. Miyahara *et al.*, Prog. Theor. Phys. Suppl. **168**, 90 (2007).
[3] I. Jaegle *et al.* [CBELSA and TAPS Collaborations], Phys. Rev. Lett. **100**, 252002 (2008).
[4] I. Jaegle *et al.*, Eur. Phys. J. A **47**, 89 (2011).
[5] D. Werthmüller *et al.* [A2 Collaboration], Phys. Rev. Lett. **111**, 232001 (2013).
[6] L. Witthauer *et al.* [A2 Collaboration], Eur. Phys. J. A **49**, 154 (2013).
[7] D. Werthmüller *et al.* [A2 Collaboration], Phys. Rev. C **90**, 015205 (2014).
[8] O. Bartalini *et al.* [GRAAL Collaboration], Eur. Phys. J. A **33**, 169 (2007).
[9] E. F. Nicoll *et al.* [Crystal Ball at MAMI Collaboration], Phys. Rev. C **82**, 035208 (2010) Erratum: [Phys. Rev. C **84**, 029901 (2011)].
[10] L. Witthauer *et al.* [A2 Collaboration], Phys. Rev. Lett. **117**, 132502 (2016).
[11] V. Kuznetsov *et al.*, Acta Phys. Polon. B **39**, 1949 (2008).
[12] V. Shklyar, H. Lenske and U. Mosel, Phys. Lett. B **650**, 172 (2007).
[13] R. Shyam and O. Scholten, Phys. Rev. C **78**, 065201 (2008).
[14] A. V. Anisovich, I. Jaegle, E. Klempt, B. Krusche, V. A. Nikonov, A. V. Sarantsev and U. Thoma, Eur. Phys. J. A **41**, 13 (2009).
[15] A. V. Anisovich, E. Klempt, B. Krusche, V. A. Nikonov, A. V. Sarantsev, U. Thoma and D. Werthmüller, Eur. Phys. J. A **51**, 72 (2015).
[16] M. Döring and K. Nakayama, Phys. Lett. B **683**, 145 (2010).
[17] K. S. Choi, S. i. Nam, A. Hosaka and H.-Ch. Kim, Phys. Lett. B **636**, 253 (2006).
[18] K. S. Choi, S. i. Nam, A. Hosaka and H.-Ch. Kim, J. Phys. G **36**, 015008 (2009).
[19] J.-M. Suh, S.-H. Kim, and H.-Ch. Kim, in preparation (2018).
[20] V. Kuznetsov *et al.*, Pisma Zh. Eksp. Teor. Fiz. **105**, 591 (2017).
[21] V. Kuznetsov *et al.*, Phys. Rev. C **83**, 022201(R) (2011).
[22] V. Kuznetsov *et al.*, Phys. Rev. C **91**, 042201 (2015).
[23] V. Kuznetsov *et al.*, JETP Lett. **106**, 693 (2017) [Pisma Zh. Eksp. Teor. Fiz. **106**, 667 (2017)].
[24] A. Gridnev *et al.* [EPECUR Collaboration], Phys. Rev. C **93**, 062201 (2016).
[25] D. Werthmüller, L. Witthauer, D. I. Glazier and B. Krusche, Phys. Rev. C **92**, 069801 (2015).
[26] T. Mart, Phys. Rev. D **83**, 094015 (2011).
[27] T. Mart, Phys. Rev. D **88**, 057501 (2013).
[28] T. Mart, A. Rusli, PTEP **2017**, 123D04 (2017).
[29] Y. Tsuchikawa *et al.*, JPS Conf. Proc. **10**, 032010 (2016).

- [30] Y. Tsuchikawa *et al.*, JPS Conf. Proc. **17**, 062007 (2017).
- [31] N. Compton *et al.*, CLAS Collaboration, Phys. Rev. C **96**, 065201 (2017).
- [32] D. H. Ho *et al.*, CLAS Collaboration, arXiv:1805.04561 [nucl-ex].
- [33] S.-H. Kim and H.-Ch. Kim, to appear in Phys. Lett. B (2018) arXiv:1806.01992 [hep-ph].
- [34] M. V. Polyakov and A. Rathke, Eur. Phys. J. A **18**, 691 (2003).
- [35] D. Diakonov, V. Y. Petrov and P. V. Pobylitsa, Nucl. Phys. B **306**, 809 (1988).
- [36] C. V. Christov, A. Blotz, H.-Ch. Kim, P. Pobylitsa, T. Watabe, T. Meissner, E. Ruiz Arriola and K. Goeke, Prog. Part. Nucl. Phys. **37**, 91 (1996).
- [37] D. Diakonov, hep-ph/9802298.
- [38] H.-Ch. Kim, M. Polyakov, M. Praszalowicz, G. S. Yang and K. Goeke, Phys. Rev. D **71**, 094023 (2005).
- [39] H.-Ch. Kim, G. S. Yang and K. Goeke, Prog. Theor. Phys. Suppl. **168**, 62 (2007).
- [40] G. S. Yang and H.-Ch. Kim, PTEP **2013**, 013D01 (2013).
- [41] M. Praszalowicz and K. Goeke, Phys. Rev. D **76**, 096003 (2007).
- [42] M. Tanabashi *et al.* [Particle Data Group], Phys. Rev. D **98**, 030001 (2018).
- [43] T. Nakano *et al.* [LEPS Collaboration], Phys. Rev. C **79** (2009), 025210.
- [44] G. S. Yang and H.-Ch. Kim, Prog. Theor. Phys. **128**, 397 (2012).
- [45] V. V. Barmin *et al.* [DIANA Collaboration], Phys. Rev. C **89**, no. 4, 045204 (2014) [arXiv:1307.1653 [nucl-ex]].
- [46] T. Sekihara, H.-Ch. Kim, and A. Hosaka, in preparation.
- [47] C. Alt *et al.* [NA49 Collaboration], Phys. Rev. Lett. **92**, 042003 (2004) [hep-ex/0310014].
- [48] G. S. Yang and H.-Ch. Kim, J. Korean Phys. Soc. **61**, 1956 (2012).
- [49] G. S. Yang, H.-Ch. Kim and M. V. Polyakov, Phys. Lett. B **695**, 214 (2011).
- [50] G. S. Yang and H.-Ch. Kim, Phys. Rev. C **92**, 035206 (2015).
- [51] H.-Ch. Kim, M. V. Polyakov, M. Praszalowicz and G. S. Yang, Phys. Rev. D **96**, 094021 (2017) Erratum: [Phys. Rev. D **97**, 039901 (2018)].
- [52] G. S. Yang and H.-Ch. Kim, Phys. Lett. B **781**, 601 (2018).
- [53] E. Witten, Nucl. Phys. B **223**, 422 (1983).
- [54] M. Chemtob, Nucl. Phys. B **256**, 600 (1985).
- [55] P. O. Mazur, M. A. Nowak and M. Praszalowicz, Phys. Lett. B **147**, 137 (1984).
- [56] S. Jain and S. R. Wadia, Nucl. Phys. B **258**, 713 (1985).
- [57] A. Blotz, D. Diakonov, K. Goeke, N. W. Park, V. Petrov and P. V. Pobylitsa, Nucl. Phys. A **555**, 765 (1993).
- [58] J. Gasser and H. Leutwyler, Phys. Rept. **87**, 77 (1982).
- [59] H.-Ch. Kim, M. V. Polyakov, M. Praszalowicz and K. Goeke, Phys. Rev. D **57**, 299 (1998).
- [60] H.-Ch. Kim, M. Praszalowicz and K. Goeke, Phys. Rev. D **57**, 2859 (1998).
- [61] G. S. Yang and H.-Ch. Kim, Phys. Lett. B **785**, 434 (2018).
- [62] H. J. Behrend *et al.* [CELLO Collaboration], Z. Phys. C **49**, 401 (1991).
- [63] A. Bramon, R. Escribano and M. D. Scadron, Eur. Phys. J. C **7**, 271 (1999).
- [64] K. Goeke, M. V. Polyakov and M. Praszalowicz, Acta Phys. Polon. B **42**, 61 (2011) [arXiv:0912.0469 [hep-ph]].